

## Comparing and Correlating Solubility Parameters Governing the Self-Assembly of Molecular Gels Using 1,3:2,4-Dibenzylidene Sorbitol as the Gelator

Yaqi Lan,<sup>†</sup> Maria G. Corradini,<sup>†</sup> Xia Liu,<sup>‡</sup> Tim E. May,<sup>‡</sup> Ferenc Borondics,<sup>‡</sup> Richard G. Weiss,<sup>§</sup> and Michael A. Rogers\*,<sup>†</sup>

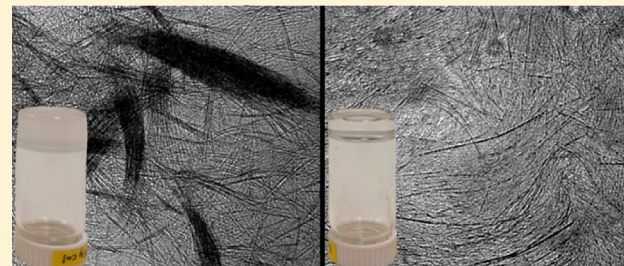
<sup>†</sup>School of Environmental and Biological Sciences, Rutgers University, New Brunswick, New Jersey 08901, United States

<sup>‡</sup>Canadian Light Source, Saskatoon, SK S7N 0X4, Canada

<sup>§</sup>Department of Chemistry and Institute for Soft Matter Synthesis and Metrology, Georgetown University, Washington, DC 20057, United States

### Supporting Information

**ABSTRACT:** Solvent properties play a central role in mediating the aggregation and self-assembly of molecular gelators and their growth into fibers. Numerous attempts have been made to correlate the solubility parameters of solvents and gelation abilities of molecular gelators, but a comprehensive comparison of the most important parameters has yet to appear. Here, the degree to which partition coefficients ( $\log P$ ), Henry's law constants (HLC), dipole moments, static relative permittivities ( $\epsilon_r$ ), solvatochromic  $E_T(30)$  parameters, Kamlet-Taft parameters ( $\beta$ ,  $\alpha$ , and  $\pi$ ), Catalan's solvatochromic parameters (SPP, SB, and SA), Hildebrand solubility parameters ( $\delta_i$ ), and Hansen solubility parameters ( $\delta_p$ ,  $\delta_d$ ,  $\delta_h$ ) and the associated Hansen distance ( $R_{ij}$ ) of 62 solvents (covering a wide range of properties) can be correlated with the self-assembly and gelation of 1,3:2,4-dibenzylidene sorbitol (DBS) gelation, a classic molecular gelator, is assessed systematically. The approach presented describes the basis for each of the parameters and how it can be applied. As such, it is an instructional blueprint for how to assess the appropriate type of solvent parameter for use with other molecular gelators as well as with molecules forming other types of self-assembled materials. The results also reveal several important insights into the factors favoring the gelation of solvents by DBS. The ability of a solvent to accept or donate a hydrogen bond is much more important than solvent polarity in determining whether mixtures with DBS become solutions, clear gels, or opaque gels. Thermodynamically derived parameters could not be correlated to the physical properties of the molecular gels unless they were dissected into their individual HSPs. The DBS solvent phases tend to cluster in regions of Hansen space and are highly influenced by the hydrogen-bonding HSP,  $\delta_h$ . It is also found that the fate of this molecular gelator, unlike that of polymers, is influenced not only by the magnitude of the distance between the HSPs for DBS and the HSPs of the solvent,  $R_{ij}$ , but also by the directionality of  $R_{ij}$ : if the solvent has a larger hydrogen-bonding HSP (indicating stronger H-bonding) than that of the DBS, then clear gels are formed; opaque gels form when the solvent has a lower  $\delta_h$  than does DBS.



### INTRODUCTION

Self-assembly utilizing hierarchical processes is an attractive approach for constructing complex supramolecular nanostructures that spontaneously produce ordered ensembles of the molecular components. However, mechanisms governing the self-assembly of many molecular nanostructures, including molecular gels, are poorly understood.<sup>1,2</sup> The vast majority of molecular gels spontaneously form self-assembled networks (i.e., self-assembled fibrillar networks, SAFiNs) via an aggregation–nucleation–growth pathway. Because the self-assembly process for molecular gels and numerous other architectures is dependent on solvent properties/structures, vicinal solvent molecules must play an explicit role in mediating the aggregation of initially dissolved gelator molecules and their growth into fibers.<sup>3</sup>

For almost 125 years, since Ostwald made one of his many prophetic statements, it has been known that chemical processes in nature occur predominantly in solution.<sup>4</sup> Also, any chemical process taking place in solution, including aggregation or crystal growth, is affected by the properties of the solution.<sup>5</sup> Due to the solvent–gelator interplay, numerous attempts have been made to correlate solvent parameters and gelation ability.<sup>6–8</sup> Since self-assembly is influenced by both solvent–solute interactions and bulk solvent properties such as viscosity and chemical potential, it is almost impossible to know *a priori* which solvent parameters will lead to the desired self-assembly.<sup>5</sup>

**Received:** March 3, 2014

**Revised:** May 20, 2014

**Published:** May 21, 2014

However, the solvent cannot be considered to be a macroscopic continuum that is characterized only by bulk physical properties during the execution of a particular process by a solute; individual solvent molecules interact differently with a solute than they do with each other and, potentially, at different points along a reaction or nucleation coordinate.<sup>9</sup> Therefore, numerous attributes of the solvent–gelator interactions must be taken into account individually in order to understand how a solvent affects the aggregation, nucleation, and growth of molecular gelators such as 1,3:2,4-dibenzylidene sorbitol (DBS). Those attributes include (i) bulk physical properties (i.e., macroscopic properties); (ii) microscopic noncovalent and solvatophobic interactions; (iii) solvation of multicomponent systems; and (iv) chemical solvation during association/dissociation processes.<sup>9</sup>

Unfortunately, no one solvent parameter accounts for all of these effects, and even polarity is a method-dependent measurement. In this regard, Katrikzky et al. stated that “the simple concept of polarity as a universally determinable and applicable solvent characteristic is a gross oversimplification”.<sup>4</sup> A true measure of solvating ability by a liquid must account for all of the factors leading to solvent–solute interactions and must separate them in a quantitative fashion according to whether they are nonspecific or specific (assuming that they do not lead to chemical transformations between the solvent and solute).

A vast majority of solvent parameters have originated historically from polymer physics, where solvent–polymer interactions dictate the solubility of a polymer and, in turn, polymer–polymer interactions. The self-assembly of molecular gels requires the same solubility considerations as for polymers and additionally the treatment of factors related to how solvents affect intermolecular, noncovalent interactions among gelator molecules. The latter must be attractive in order for the nucleation and growth of the fibers that constitute a SAFiN to occur. Thus, although two solvents may have the same static relative permittivity/polarity, their different functional groups may drastically alter the nature of their noncovalent gelator–solvent interactions. For this reason, they may not be equally amenable to gelation by a common gelator, such as DBS, and their gels may exhibit very different kinetic and mechanical properties. For example, although both 3-pentanone and 1-butanol have static relative permittivities of  $\sim 17$ ,<sup>10</sup> only 3-pentanone is gelated by 12-hydroxystearic acid (12HSA), a solution obtained in 1-butanol under otherwise equivalent conditions.<sup>11–14</sup> For this reason, detailed evaluations of how different solvent parameters alter or influence gelation are desperately needed.

The application of Hansen solubility parameters (HSPs),<sup>6,9,11–15</sup> first applied to molecular gels by Raynal and Bouteiller,<sup>6</sup> is the most frequently used method to predict when a molecular gelator will gelate a liquid. Numerous other measures of solubility have been applied as well<sup>7,8</sup> to analyze individual molecular gels.<sup>16,46,47</sup> They include dielectric constants,<sup>15</sup> Hildebrand solubility parameters,<sup>6,7</sup>  $E_T(30)$  parameters,<sup>17</sup> solvent polarity (which includes polarizability (SPP)), solvent basicity (SB), and solvent acidity (SA)),<sup>18</sup> Kamlet–Taft parameters,<sup>15</sup> and the Flory–Huggins parameter.<sup>16</sup> However, to the best of our knowledge, a comparison among (and combined use of) these diverse parameters to explain why some solvents lead to gels and others do not with one gelator (and its self-assembling characteristics) has not been made. Herein, we report the results from such a study using DBS as the gelator. DBS has been chosen because it is known to be an efficient

gelator of many solvents<sup>19</sup> and has been used in several industrial applications. We emphasize that the approach described here should be applicable to a wide range of other molecular gelators. Of course, each must be evaluated experimentally for its aggregating properties and the nature of its self-assembled materials.

## METHODS

Solvents for gelation tests (Sigma-Aldrich, St. Louis, MO, USA) were used as received (Supporting Information file, Table S1). Specific amounts of DBS (99% purity, BocSciences, New York, NY, USA) were added at 1 to 5 wt % in 1 wt % increments to a solvent and were heated in closed vials with Teflon liners (VWR, Allentown, PA, USA) in a heating block (set at 250 °C) until a clear solution/sol (by visual inspection) persisted for at least 5 min. The vial was then cooled to room temperature ( $\sim 20$  °C), except when the melting temperature of the solvent was  $>20$  °C, as for tetrahydrothiophene (mp  $\sim 26$  °C) and 1,3-dioxolan-2-one (mp  $\sim 34$ –37 °C). In those cases, the samples were incubated at 40 °C. After 24 h at an incubation temperature, each vial was inverted for 1 h. If any flow was detected, then the sample was classified as a sol. The DBS concentration was increased in 1 wt % increments, and the closed vial was reheated and recooled as before. This process was repeated until no flow was observable (i.e., the sample could be classified qualitatively as a gel) or the DBS concentration reached 5 wt %. Transparency and opacity were determined visually at the critical gelator concentration (CGC) because opacity increases with increasing concentration. The degree of opacity also depends on the difference between the refractive index of a solvent and a gelator SAFiN.

The possible gelation of 62 solvents by DBS has been investigated (Supporting Information, Table S1). The solvents were selected to give a wide range of dispersive ( $\delta_p$ ), polar ( $\delta_p$ ), and hydrogen-bonding components ( $\delta_h$ ) for the Hansen solubility parameters (HSPs).<sup>20</sup> A second criterion was that they remain liquid at the gelation temperature ( $\sim 20$  °C), with the exception of tetrahydrothiophene and 1,3-dioxolan-2-one, whose DBS mixtures were examined at 40 °C. DBS was able to gelate all but 7 of the solvents: 40 of the solvents led to clear gels and 15 yielded opaque gels. The opacity of molecular gels has been correlated previously with the morphologies of the SAFiNs, including the cross-sectional thickness and the type and number of fiber–fiber interactions, as viewed by various microscopy techniques (Supporting Information, Figures S2 and S3).<sup>21</sup> DBS has been shown recently to be as close to a universal gelator as has been achieved.<sup>22</sup> Its extensive gelation ability can be related to the molecular structure, which allows both hydrogen bond donation and acceptance as well as  $\pi$  stacking.

Rheological analyses were carried out using a TA Instruments Discovery H2 hybrid rheometer with an 8 mm stainless steel cross-hatched parallel plate geometry and a temperature-controlled stainless steel Peltier plate (New Castle, DE, USA). Due to the volatility of some of the solvents used in this study, rheological molds were made using steel compression fittings, which created a 700- $\mu\text{m}$ -thick sample with a diameter of 1200  $\mu\text{m}$  (Supporting Information, Figure S1). These compression fittings allowed the gels to be heated in the mold without solvent evaporation. Stress sweeps at 20 °C and a frequency of 1 Hz were conducted from 1 to 10 000 Pa or until the gel yielded, triggering an overspeed error.

Microstructural investigations of the solutions/sols in the seven solvents that did not yield a gel at up to 5 wt % DBS (i.e., 1-methyl-2-pyrrolidone, *N,N*-dimethylformamide, pyridine, pyridazine, 1,3-dioxolan-2-one, dimethyl sulfoxide, and tetrahydrothiophene) gave no evidence of gelator aggregates being formed (Supporting Information, Figure S2A,B). Conversely, clear (Supporting Information, Figure S2C,D) and opaque gels (Supporting Information, Figure S2E,F) had bicontinuous networks. The clear gels were composed of thinner fibers than the opaque gels, and the opaque gels tended to form large clusters of fibers that were more birefringent (Supporting Information, Figure S2E,F). The differences in birefringence may be related to variations in the molecular packing of DBS molecules or in the degree of annealing of the networks.<sup>23</sup> To avoid the possible loss of solvent during preparations, gels for imaging were preformed in vials and small

amounts were placed between the slides and coverslips (leading to thickness variations); hence, it was not possible to determine fractal values and crystal sizes within the microstructures.

## RESULTS AND DISCUSSION

**Application of Solubility Parameters to Nanoscale Assemblies.** Solvent parameters have routinely been used to assess the role of solvent in controlling the phase separation, nucleation, and crystal growth of small molecules.<sup>5</sup> Although the current study examines the role of solvents and their parameters in the assembly of small molecules, the universal underlying mechanisms have been shown to apply to polymer<sup>24</sup> and protein aggregation<sup>25</sup> and the neurodegenerative aggregation of amyloid plaques.<sup>26</sup> Also, solvent parameters have been exploited to understand and manipulate nanoscale assemblies, allowing different polymorphs of single crystals to be grown from their corresponding sols.<sup>27</sup> The formation of different crystalline polymorphs from sols is dependent not only on solvent–solute interactions on molecular level but also on the macroscopic bulk properties, including surface tension and viscosity.<sup>5</sup> Because of the interplay between parameters, it becomes extraordinarily difficult to select a single solvent parameter either to predict or to understand the effect of a solvent on the self-assembly of solute molecules.

**Bulk Physical Polarity Scales.** Frequently, and most simply, solvents are characterized by their bulk properties. These include polarity, assessed using partition coefficients (log  $P$ ) (Figure 1A);

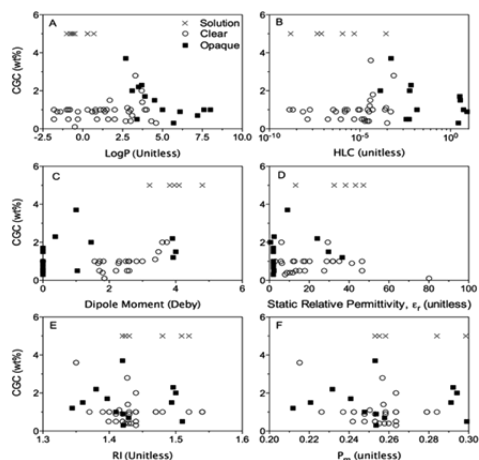


**Figure 1.** Critical gelator concentrations (CGCs) of DBS in various organic solvents versus octanol–water partition coefficients (A),<sup>10</sup> Henry's law constants (B),<sup>30</sup> dipole moments (C),<sup>10</sup> static relative permittivities (D),<sup>10</sup> refractive indexes (RI) (E),<sup>32</sup> and the molar polarization ( $P_m$ ) (F) of the solvents.

Henry's law constants, HLCs, (air–water equilibrium partition coefficients) (Figure 1B);<sup>28</sup> dipole moments (arising from the nonuniform distributions of atomic charges) (Figure 1C); static relative permittivities/dielectric constants (the ratio of the amount of electrical energy stored in a material by an applied voltage relative to that stored in a vacuum) (Figure 1D); and refractive indexes (the velocity of light in a solvent compared to that in a vacuum) (Figure 1E).

**Partition Coefficients and Henry's Law Constants.** Determining how a pure substance distributes itself between two partially miscible solvents, such as 1-octanol and water, which are in intimate contact is the basis of the partition coefficient parameter, log  $P$  (eq 1).<sup>28</sup>

$$\log P = \log \left( \frac{[X_{C_8H_{18}O}^{\text{organic}}]}{[X_{H_2O}^{\text{aqueous}}]} \right) \quad (1)$$

Here,  $X$  is the mole fraction of the solvent in each phase. Figure 1A illustrates that elevated CGCs occur in solvents with intermediate values of  $P$  ( $\sim 10^{2.5}$ ),<sup>29</sup> while the ability to self-assemble is not restricted to any region of  $P$  (i.e., clear gels form in low-polarity solvents and opaque gels are observed in high-polarity solvents). CGC is a widely used parameter in assessing the role of solvent in the mechanism of self-assembly due to its wide variability and ease of measurement. Although gel opacity and CGC seem to correlate with the solvent partition coefficients, the ability to differentiate solvents capable of promoting self-assembly or that facilitate solvation do not have a clear relationship.

Henry's law constants (HLCs) are limiting Gibbs energy quantities and they are influenced by the same factors associated with the log  $P$  constants.<sup>28</sup> Instead of measuring the partitioning between two liquid phases, HLCs measure the volatility of compounds or the water-to-air partition, which are a function of the intermolecular interactions between solvent molecules.<sup>30</sup> Although HLCs can be represented in numerous formats, the air-to-water ratio on a mole or weight per unit volume basis is used for the purpose of this study and results in a unitless mass distribution (eq 2).

$$\text{HLC} = \frac{C_{i,G}}{C_{i,L}} \quad (2)$$

$C_{i,G}$  is the concentration of the solvent on a mass per unit volume basis, and G and L denote the gas and liquid phases, respectively.<sup>30</sup> As expected, the trends observed for HLCs<sup>29</sup> (Figure 1B) are similar those observed for the partitioning coefficients (Figure 1A).

**Dipole Moments.** Even though they vary with temperature and molecular conformation,<sup>10</sup> dipole moments were roughly able to differentiate solvents that yield opaque and clear gels as well as those that led to solutions (Figure 1C). However, this parameter did not unambiguously classify the gels. The dipole moments of three short-chained nitriles examined (acetonitrile, propanenitrile, and butanenitrile) resided at the interface between the regions of clear gel and solution phases. Upon careful inspection, it was found that the DBS samples in these nitriles contain regions that were transparent with opaque clusters. Also, the dipole moments of all of the solvents which formed clear gels with DBS and had a CGC higher than 2 wt % reside between 3D and 4D; the dipole moments of most of the solvents that formed solutions with DBS were >4D.

**Static Relative Permittivities.** Dielectric constants<sup>10</sup> have been used routinely to assess how physical properties of molecular gels change as a function of solvent properties.<sup>12,15</sup> These studies illustrate that within a class of solvents which have the same functional groups (e.g., alcohols of differing alkyl chain length) the physical properties (i.e., sol–gel transition temperature<sup>15</sup> or CGC<sup>12</sup>) correlate in a linear fashion with the dielectric constant. However, no correlations were found here between the dielectric constants of solvents and the physical properties of their DBS gels or the ability of the solvents to form a gel (Figure 1D). The lack of correlations here is not surprising because it has been established that dielectric constants are an incomplete measure of solvent polarity.<sup>31</sup> Although, as noted above, simple assessments of polarity seem to aid in understanding the differences between the opacity and transparency of molecular

gels (i.e., more polar solvents produced transparent DBS gels), they do not provide deep insights into why SAFeNs are formed in some solvents and not in others.

**Refractive Index.** The refractive index,  $n$ , of a solvent is utilized to calculate its molar polarization,  $P_m$ , by the Lorenz–Lorentz equation (eq 3):

$$P_m = \frac{(n^2 - 1)}{(n^2 + 2)} \quad (3)$$

Both the refractive index and the molar polarization of a solvent are dependent on its polarizability and molar mass. Neither parameter seems to be critical in dictating the gelation behavior of DBS (Figure 1E,F). This finding is consistent with the aforementioned observations employing static relative permittivities, which scale in a nonexponential fashion with the refractive index (eq 4).

$$n = \epsilon_r^{1/2} \quad (4)$$

**Conclusions about Gel Properties from Bulk Physical Properties of the Solvents.** It has been argued previously that macroscopic properties such as the refractive index and static relative permittivities are not suitable measures of molecular–microscopic interactions.<sup>33</sup> Considering a solvent to be a macroscopic continuum, characterized by a single physical constant (e.g., dipole moment, dielectric constant, refractive index, etc.) is insufficient to predict gelation behavior. Parameters that are capable of predicting gelation must consider the solvent to be a discontinuous phase consisting of individual, mutually interacting molecules. In this regard, the limitations to physical measures of polarity have been shown experimentally: in general, the static relative permittivity, in the vicinity of a solute, is lower than that of the bulk because solvent dipoles in the solvation shell are more constrained.<sup>33</sup> These discrepancies have led to the development of spectroscopic measures of solvent polarity that are sensitive to specific solvent–solute microscopic interactions and thus are more likely to correlate with different aspects of self-assembly in molecular gels.

**Solvatochromic Solvent Parameters.** The aforementioned electrostatic models involving dielectric constants, dipole moments, and so forth consider solvents simplistically as nonstructured homogeneous fluids having uniform macroscopic properties. They do not consider microscopic inhomogeneities and specific intermolecular interactions.<sup>34</sup> To understand the nature of SAFeN formation, solute–solvent interactions, which occur on the molecular-to-microscopic levels and involve solvation shells, must be considered.<sup>34</sup> The electrostatic models do not account for acid–base interactions, donor–acceptor complexation, or the strengths of Keesom, Debye, and London dispersion forces.

However, solvatochromic parameters assess the polarity using solvent-sensitive compounds that absorb and/or emit radiation. The absorption spectra of such compounds are sensitive to their environments, and the degree to which their spectral characteristics change is associated with the nature of the local solvation shell.<sup>4</sup>

**$E_T(30)$  Scale.** Reichardt's  $E_T(30)$  parameter utilizes the overall solvation capability of reporter molecules in both their electronic ground and excited states to define solvent polarity.<sup>31</sup>  $E_T(30)$  parameters account for all possible (specific and nonspecific) intermolecular forces between solvent and solute molecules (i.e., Coulomb interactions present between ions, directional interactions between dipoles, and inductive, dis-

persion, hydrogen-bonding, and charge-transfer forces as well as solvophobic interactions) without separating them into their components.<sup>9</sup> One major limitation of the  $E_T(30)$  scale is its inapplicability to systems that undergo chemical reactions, such as condensations or hydrolyses.<sup>9</sup> To overcome the nonspecific nature of the aforementioned methods, the molar electronic transition energies of negatively charged solvatochromic dye pyridinium (2,6-diphenyl-4-(2,4,6-triphenylpyridinium-1-yl)-phenolate) (Figure 2A), expressed as ( $E_T(30)$ , eqs 5–7), have

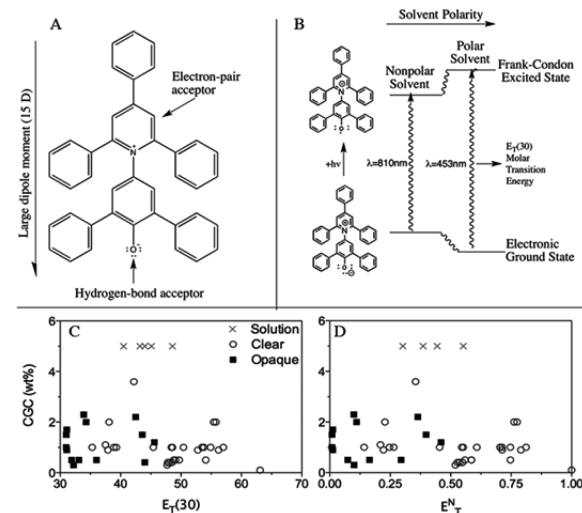


**Figure 2.** Chemical structure and ground-state properties of 2,6-diphenyl-4-(2,4,6-triphenylpyridinium-1-yl)phenolate (A), and the influence of solvent polarity on its intramolecular charge-transfer transition with the electronic transition energies (B), adapted from Reichardt.<sup>34</sup> CGCs as a function of both  $E_T(30)$  (C) and  $E_T^n$  (D) parameters. Solutions are assigned a CGC of 5 for graphical representation.

been used as a probe of solvent polarity properties (Figure 2B) (eqs 5–7):<sup>35</sup>

$$E_T(30) = hc\nu_{\max} N_A \quad (5)$$

$$E_T(30) = (2.8591 \times 10^{-3})\nu_{\max}(\text{cm}^{-1}) \quad (6)$$

$$E_T(30) = (28591/\lambda_{\max})(\text{nm}^{-1}) \quad (7)$$

Here,  $\nu_{\max}$  is the wavenumber and  $\lambda_{\max}$  is the wavelength of the intensity maximum of the longest-wavelength absorption band of the dye, an intramolecular  $\pi-\pi$  charge-transfer transition.<sup>34</sup> This scale is often converted to a dimensionless value using the molar electronic transition energy of two reference solvents, water ( $E_T^n = 1$ ) and tetramethylsilane (TMS) ( $E_T^n = 0$ ) (eq 8).

$$E_T^n = \frac{[E_T(\text{solvent}) - E_T(\text{TMS})]}{[E_T(\text{water}) - E_T(\text{TMS})]} \quad (8)$$

$E_T^n(30)$  values cannot always be determined for low-polarity solvents, such as alkanes, due to the poor solubility of betaine dyes in them. Interestingly, the  $E_T(30)$  and  $E_T^n$  parameters are ineffective at predicing DBS gel formation (Figure 2C,D), suggesting that the self-assembly of these molecular gels is not dependent solely on solvent polarizability, irrespective of whether polarity is measured using microscopic- or macroscopic-sensitive methods.  $E_T(30)$  is interpreted to be a measure of the overall solvating capacity of the solvent, accounting for all nonspecific and specific intermolecular solute–solvent inter-

actions. In addition, the molecular self-recognition between DBS molecules that drives self-assembly and is time-dependent must influence solvent–solute interactions. The manner in which a solvent interacts in the various stages of DBS (or any other molecular gelator) aggregation, along the path to SAFiN formation, may change.

**Kamlet–Taft Parameters.** Kamlet–Taft parameters are an extension of the  $E_T(30)$  parameter. They utilize a series of probes which undergo solvatochromic shifts sensitive to different aspects of solvent polarity and solvent–solute interactions. The advantage of Kamlet–Taft parameters is that they dissect solvent polarity into general and specific interactions.<sup>36–38</sup> General interactions (expressed by the dipolarity/polarizability parameter,  $\pi$ ) originate from electrostatic and dispersive interactions, related conceptually to reaction field theories.<sup>4,39–41</sup> The specific interactions include hydrogen-bond donating (the acidity parameter,  $\alpha$ ) and hydrogen-bond accepting (the basicity parameter,  $\beta$ ) terms.<sup>4,39–41</sup> These parameters were first applied to molecular gels with L-lysine bis-urea gelators, where it was found that the  $\alpha$  parameter was of primary importance and its magnitude could be correlated with the ability of the gelator to establish a hydrogen-bonded network.<sup>41</sup> The  $\beta$  and  $\pi$  parameters participated in subsidiary roles: the magnitude of  $\beta$  affected the stability of the gel, and  $\pi$  indicated the influence of fiber–fiber interactions.<sup>41</sup>

**Dipolarity/Polarizability Parameter.** The dipolarity/polarizability  $\pi$  parameter is a combined measure of solvent polarity and polarizability or the nonspecific portion of the van der Waals interactions between the solvent and solute. It is obtained using the spectra of either *p*-nitroanisole or *N,N*-dimethyl-*p*-nitroaniline (NNDN) (Figure 3A) according to eq 9:<sup>39</sup>

$$\pi = \frac{\nu - 28.18}{-3.52} \quad (9)$$

$\nu$  is the frequency maximum of the NNDN UV-vis absorption band ( $\text{cm}^{-1}$ ), and the constants ( $\text{cm}^{-1}$ ) arise from the normalization of the  $\pi$  parameter between 0.0 for cyclohexane and 1.0 for DMSO.<sup>36</sup> Competing intermolecular forces establish the conformation of NNDN, where steric repulsion favors nonplanar conformations (Figure 3A left) and resonance structures favor a planar conformation (Figure 3A right).<sup>36</sup> Changes in spectral features arise because of solvent-induced changes in the angles of nonplanarity: more-polar solvents stabilize the charge-separated, quinoid (planar) resonance structure better (Figure 3A right).<sup>36</sup> Similar to other measures of solvent polarity (i.e.,  $E_T(30)$ ,  $\log P$ , HLCs, and  $D$  and  $\epsilon$  values), the  $\pi$  parameter was unable to distinguish solutions from clear molecular gels of DBS (Figure 3D). However, it did show a stark difference between opaque gels, found in low-polarity solvents, and clear gels that form in high-polarity solvents. The advantage of the  $\pi$  scale is that it accounts for the type of molecular polarization that occurs during the 1D assembly of DBS molecules. Polarization occurs whether DBS forms intermolecular or intramolecular H-bonds.

**Solvent Basicity Scale.** The  $\beta$  parameter is specific to solute–solvent interactions, where the solute plays the role of an electron-pair acceptor and the solvent is an electron-pair donor.<sup>4</sup> It is determined using the difference in the wavenumbers of the intensity maximum of the absorption bands between *p*-nitrophenol ( $\nu_2$ ) and the non-hydrogen-bond-accepting molecule, NNDN ( $\nu_1$ ) (eq 10).<sup>39</sup>

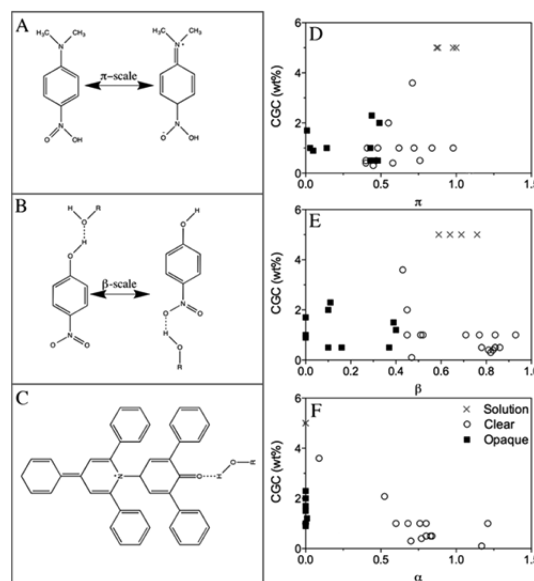


**Figure 3.** Kamlet–Taft solvatochromic parameters, including the dipolarity/polarizability ( $\pi$  parameter) using *N,N*-dimethyl-*p*-nitroaniline (A), the basicity or hydrogen-bond-accepting parameter using *p*-nitroaniline ( $\beta$  parameter) (B), and the acidity or hydrogen-bond-donating parameter ( $\alpha$  parameter) using the Dimroth–Reichardt betaine dye (C). Kamlet–Taft solvatochromic parameters  $\pi$  (D),  $\beta$  (E), and  $\alpha$  (F) as a function of the CGCs. Solutions are assigned a CGC of 5 for graphical representation.

$$\beta = \frac{0.9841\nu_1 + 3.49 - \nu_2}{2.759} \quad (10)$$

The constants (in  $\text{cm}^{-1}$ ) arise from a standardized value of 1 for hexamethylphosphoramide.<sup>39</sup> If a solvent acts as a hydrogen-bond acceptor, then the electronic transition from a hydrogen-bonded ground state (Figure 3B left) to an excited state (Figure 3B right) increases the strength of the hydrogen bond in the excited state and lowers the transition energy.<sup>37</sup> The  $\beta$  value seems to be an extremely important parameter in predicting the gelation of DBS (Figure 3D): DBS formed solutions in solvents with  $\beta$  values of between 0.5 and 0.8 and clear gels in the ranges of  $0.4 < \beta < 0.5$  and  $\beta > 0.7$ . When the  $\beta$  parameter is less than 0.4, opaque gels result without exception. There is extremely little overlap of regions of the different DBS phases, suggesting that the ability of the solvent to accept a hydrogen bond is a central property in dictating the microstructure and ability of DBS to form gels.

**Solvent Acidity Scale.** Equal in importance to hydrogen-bond acceptance in predicting the ability of DBS to self-assemble into a SAFiN is hydrogen-bond donation, as measured by the  $\alpha$  parameter. The  $\alpha$  parameter is determined by the difference in the wavenumbers for the maximum intensities of the absorption bands for the Dimroth–Reichardt betaine dye ( $\nu_3$ ) (Figure 3C) and NNDN ( $\nu_1$ ) (Figure 3C) (eq 11).

$$\alpha = \frac{1.873\nu_1 - 74.58 + \nu_3}{5.47} \quad (11)$$

The constants (in  $\text{cm}^{-1}$ ) are based upon a standardized value of 1 for methanol.<sup>38</sup> The  $\alpha$  parameter arises from the negative solvatochromic shift due to the charge delocalization from the phenoxide oxygen into the pyridinium ring and the phenyl groups (Figure 3C).<sup>38</sup> Our results indicate that the inability to donate a hydrogen bond strongly impedes SAFiN formation of

DBS in clear organogels (Figure 3F). When a solvent cannot donate a hydrogen bond (i.e.,  $\alpha = 0.0$ ), DBS forms either a solution or an opaque gel. The same conclusion was reached for L-lysine bis-urea gels.<sup>41</sup> Clear molecular gels resulted when  $\alpha$  was  $\gtrsim 0$ .

**Catalan's Solvent Scales.** Catalan et al. utilized solvatochromic techniques similar to those used for Dimroth and Reichardt's  $E_T(30)$  and Kamlet–Taft's  $\alpha$ ,  $\beta$ , and  $\gamma$  parameters.<sup>42–44</sup> The difference between Catalan's and Kamlet–Taft's parameters is that they utilize different series of probe and homomorph molecules. Each pair of probes is used to determine the solvent dipolarity/polarizability (SPP), solvent acidity (SA), and solvent basicity (SB).

**SPP Parameter.** SPP is determined using the long-wavelength absorption of 2-(dimethylamino)-7-nitrofluorene (DMANF) and its homomorph, 2-fluoro-7-nitrofluorene (FNF).<sup>42</sup> DMANF is a probe of dipolarity/polarizability because its absorption and emission spectra are sensitive to solvent polarity as a result of an increase in its dipole moment when going from the ground to the excited state (Figure 4A).<sup>42</sup> Homomorph FNF

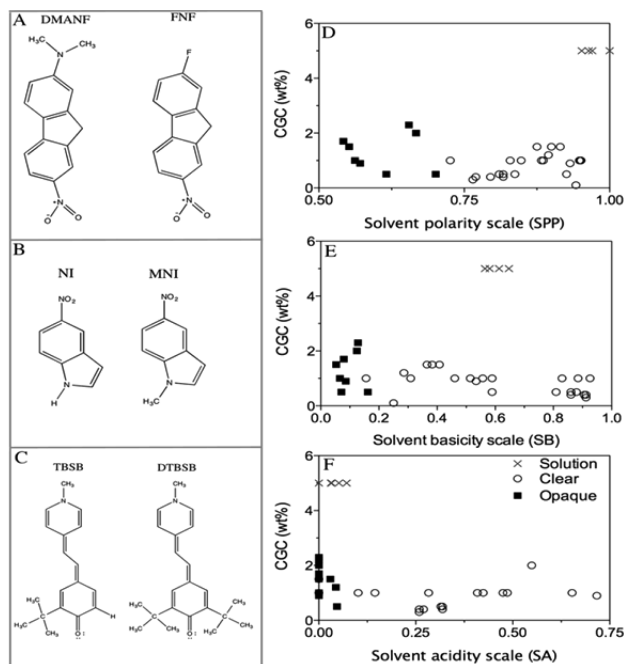


**Figure 4.** Catalán's solvatochromic parameters, including the solvent polarity scale (SPP parameter) using 2-(dimethylamino)-7-nitrofluorene (DMANF) and its homomorph, 2-fluoro-7-nitrofluorene (FNF) (A); the basicity or hydrogen-bond-accepting parameter using 5-nitroindoline (NI) and the acidic probe and its nonacidic homomorph, 1-methyl-5-nitroindoline (MNI) (B); and the acidity or hydrogen-bond-donating parameter (SA parameter) using the *o*-*tert*-butylstilbazolium betaine dye (TBSB) and its nonbasic homomorph, *o*,*o*'-di-*tert*-butylstilbazolium betaine dye (DTBSB) (C). Catalán's solvatochromic parameters, SPP (D), SB (E), and SA (F), as a function of the CGCs. Solutions are assigned a CGC of 5 for graphical representation.

has a similar structure (i.e., with a nitro group at position 7 and an electron-releasing group at position 2) but a much lower dipole moment in the ground state as a result of replacing the strongly electron-donating dimethylamino group of DMANF with a strongly electron-withdrawing fluorine atom (Figure 4A). Using the difference between the maxima of the lowest-energy

absorption bands for DMANF and FNF ( $\Delta\nu$ ), SPP is determined for a solvent using the values in DMSO and cyclohexane as references (eq 12).

$$\text{SPP} = \frac{\Delta\nu_{(\text{solvent})} - \Delta\nu_{(\text{cyclohexane})}}{\Delta\nu_{(\text{DMSO})} - \Delta\nu_{(\text{cyclohexane})}} \quad (12)$$

According to the SPP values, DBS tends to cluster the solvents that form solutions, clear gels, and opaque gels (Figure 4D). Similar to the observations from the  $E_T(30)$  parameter (Figure 2C,D) and Kamlet–Taft's  $\pi$  parameter (Figure 3D), solutions formed in the highest polarity/polarizability solvents and opaque gels occurred in the lowest-polarity solvents. Solvent polarity will affect the chemical potential difference between the solvent and initially formed DBS crystals. If the chemical potential difference between a solvent and DBS is high, then the interfacial free energy will also be elevated, causing a higher driving force for phase separation between the two phases and resulting in thicker bundles of fibers (i.e., opaque gels). Conversely, if the chemical potential difference is extremely low, then DBS will remain in solution; at intermediate differences in chemical potential, DBS will phase-separate into SAFiNs. However, the interfacial free energy will be lower, allowing DBS to form clear gels composed of small fibers with extremely high interfacial areas. From the data obtained, DBS appears to have a  $\pi$  parameter value of close to 1, where the solvents that form DBS sols reside.

The turbidity or transparency of an organogel has been correlated with the cross-sectional thickness of the crystalline aggregates, the number of junction zones capable of diffracting light, and the number of crystalline aggregates within the SAFiN.<sup>21</sup> The solvent–gelator interactions weaken gelator–gelator intermolecular hydrogen-bonding interactions, resulting in thicker crystalline fibers, and as the strength of the solvent–gelator interactions increases further, they will eventually impede the gelator–gelator interactions completely and facilitate dissolution.<sup>18</sup> Also, there was no overlap between the regions in the SPP parameter map for the different gel and solution phases. As found previously,<sup>22</sup> the opaque gels, with thicker fibers, were found in the lower-polarity solvents.

**SB Parameter.** The SB parameter of Catalán et al. is determined using acidic probe molecule 5-nitroindoline (NI) and its nonacidic homomorph, 1-methyl-5-nitroindoline (MNI) (Figure 4B).<sup>43</sup> NI is acidic in its electronic ground state, and its acidity increases in its excited singlet state. As a result, its absorption maximum is bathochromically shifted in basic media.<sup>43</sup> The selected homomorph, MNI, has a structure similar to that of NI, but it lacks the amino group. Then, the SB parameter for a solvent is determined by eq 13.

$$\text{SB} = \frac{\Delta\nu_{(\text{solvent})} - \Delta\nu_{(\text{gas})}}{\Delta\nu_{(\text{TMG})} - \Delta\nu_{\text{gas}}} \quad (13)$$

Here,  $\Delta\nu_{(\text{solvent})}$  is the difference between the maxima of the lowest-energy absorption bands between 350 and 400 nm for NI and MNI,  $\Delta\nu_{(\text{TMG})}$  is the difference between the lowest-energy absorption bands for NI and MNI in tetramethylguanidine (TMG), and  $\Delta\nu_{\text{gas}}$  is the lowest-energy absorption band in a series of *n*-alkanes and in extrapolating the Lorenz–Lorentz function ( $f(n^2) = (n^2 - 1)/(n^2 + 1)$ ) to  $n = 0$ <sup>42,45</sup> (because the probe and homomorph have not been measured directly in the gas phase). Similar to the Kamlet–Taft  $\beta$  parameter, the SB parameter shows an intermediate region of solvents that formed solutions with DBS ( $0.6 < \text{SB} < 0.8$ ) (Figure 6E). The solution

phase is flanked on either side by DBS/solvent systems that formed clear gels ( $0.2 < SB < 0.6$  and  $0.8 < SB < 1.0$ ). When  $SB < 0.2$ , opaque gels resulted.

**SA Parameter.** The SA parameter is measured using a basic probe (*o*-*tert*-butylstilbazonium betaine, TBSB) and its nonbasic homomorph (*o*,*o*-di-*tert*-butylstilbazonium betaine, DTBSB) (Figure 4C). The SA scale is set at 0.2 for ethanol (eq 14).

$$SA = \frac{\Delta\nu_{(\text{solvent})}}{1299.9} \times 0.4 \quad (14)$$

At the other extreme of the scale are solvents that are non-hydrogen-bonding. Catalan et al. utilized ~50 solvents to determine an average value, which is the zero reference point used to derive the constants (in  $\text{cm}^{-1}$ ). Applications of the Catalan SB parameter (Figure 4F) and the Kamlet-Taft  $\alpha$  parameter (Figure 3F) lead to very similar results: the opaque DBS gels and DBS solutions occurred essentially at  $SA < 0.1$ ; clear gels formed when  $SA$  is  $>1$ .

**Conclusions from Application of the Solvatochromic Parameters.** The data from the application of these solvatochromatic parameters indicate that, although solvent polarity is important, specific interactions determine the likelihood of gel formation. Also, a new important insight into the manner of aggregation of DBS is derived from these analyses: clear gels are formed in solvents unable to accept a hydrogen bond and solutions or opaque gels form in solvents that can.

**Thermodynamically Derived Solvent Parameters.** The influence of a solvent on a chemical equilibrium is determined by the standard molar Gibbs energy of solvation for solutes. Thermodynamically, either or both of the components of the molar Gibbs energy of mixing  $\Delta G_m$  and the enthalpy  $\Delta H_m$  or entropy term  $T\Delta S_m$  (or both) can be used to define the parameters for solvation.

**Hildebrand Solubility Parameters.** For polymer dissolution, enthalpy is the controlling factor in the Gibbs free energy change because only minor increases in entropy occur usually. Thus, the Hildebrand solubility parameter, as proposed in two seminal papers by Hildebrand and Scott<sup>46</sup> and Scatchard,<sup>47</sup> relies solely on enthalpy (eq 16). However, this assumption is probably not applicable to the aggregation and crystallization of small molecules such as DBS or to their self-assembly into SAFiNs because a significant change in the entropy of mixing is expected. Despite this caveat, we were interested to determine the relationship between DBS gelation and  $\Delta H_m$  as defined in eq 15.

$$\Delta H_m = V \left( \left[ \frac{\Delta E_1^v}{V_1} \right]^{1/2} - \left[ \frac{\Delta E_2^v}{V_2} \right]^{1/2} \right) \phi_1 \phi_2 \quad (15)$$

Here,  $V$  is the mixture volume,  $\Delta E_i^v$  is the energy of vaporization,  $V_i$  is the molar volume, and  $\phi_i$  is the volume fraction of component  $i$ . Under conditions of isothermal vaporization of the saturated liquid, the cohesive energy density ( $\Delta E_i^v$ ) is the negative of the energy of vaporization per  $\text{cm}^3$  of sample, corresponding to Hildebrand parameter  $\delta_i$  (eq 16).<sup>48</sup>

$$\delta_i = \left( \frac{\Delta E_i^v}{V_i} \right)^{1/2} \quad (16)$$

A correlation between the cohesive energy density (or the potential energy per unit volume) and mutual solubility is assumed.<sup>49</sup> In a condensed phase, strong attractive forces provide a negative potential energy; in the vapor phase, there is a negative

cohesive energy.<sup>49</sup> On the molecular level, the cohesive energy is a combination of the dispersion forces and polar interactions (including hydrogen bonding). The magnitudes of cohesive energy densities have been shown to be important determinants of whether a solvent will or will not promote the self-assembly of amphiphiles. The cohesive energy densities reflect the ability of a solvent to solubilize an amphiphile. They are related to the extent of intermolecular forces required to overcome solvent–solvent interactions and, as such, are thought to be a requirement for promoting amphiphile self-assembly.<sup>50</sup>

However, we find no apparent correlation between the CGCs of the gel phases of the DBS–solvent mixtures and Hildebrand solubility parameters (Figure 5A). A similar finding has been

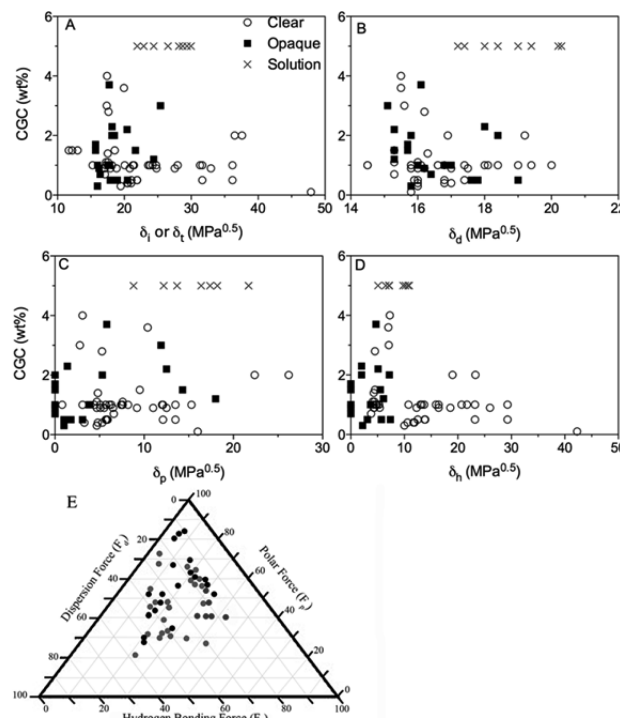


**Figure 5.** CGCs as a function of the (A) Hildebrand solubility parameter ( $\delta_T$ ) or the total Hansen solubility parameter ( $\delta_T$ ), (B) dispersive Hansen solubility parameter ( $\delta_d$ ), and (C) polar Hansen solubility parameter ( $\delta_p$ ) and (D) hydrogen-bonding Hansen solubility parameter ( $\delta_h$ ). (E) Ternary plot of calculated solubility parameters for the CGC of DBS in solvents. Black circles represent solvents that formed opaque gels, gray circles are solvents that formed clear gels, and blue circles are for DBS solutions. Solutions are assigned a CGC of 5 for graphical representation.

reported for 12HSA–solvent mixtures.<sup>12</sup> As noted above, the lack of correlations may be traced to the exclusion of entropic factors; this treatment was not designed to describe gelation/aggregation phenomena of small molecules.

**Hansen Solubility Parameters.** Major limitations of the one-component Hildebrand solubility parameter (N.B., it should be applied only to regular solutions, and it does not include molecular polarity or specific interactions<sup>49</sup>) are overcome by the multiparameter solubility term developed by Hansen.<sup>63</sup> In it, the Hildebrand parameter is separated into an atomic dispersion force, a molecular permanent dipole–dipole force, and molecular hydrogen bonding (electron-exchange) parts.<sup>19,20,48</sup> The geometric mean of the three interaction parameters for two compounds is an estimate of the interaction between two unlike

compounds in solution.<sup>51</sup> In this way, the total energy of vaporization for a liquid can be considered to consist of the three parameters mentioned above.

The dispersive interactions arise from atomic forces, typically dominated by London dispersion forces and van der Waals interactions. For saturated aliphatic hydrocarbons, the energy of vaporization is composed of only cohesive interactions ( $E_d$ ). The second part of the cohesion energy arises from permanent dipole–dipole interactions (i.e., the polar cohesive energy ( $E_p$ )). For example, because saturated fatty acids have both polar and dispersive components, both types of energies must be considered and calculated to describe how their molecules interact. The third major cohesive energy component is the hydrogen-bonding parameter ( $E_h$ ). In this simplified approach, hydrogen bonding is used to express the energies from interactions not included in the other two parameters.<sup>20</sup> Equation 17 shows the form of the HSPs as the sum of the individual total cohesion energy terms,  $E$ :<sup>20</sup>

$$E = E_d + E_p + E_h \quad (17)$$

Under conditions of isothermal vaporization of a saturated liquid, the cohesive energy density is the energy of vaporization per cm<sup>3</sup>, corresponding to the Hildebrand parameter. Dividing eq 18 by the molar volume ( $V$ ) gives eq 18 and the square of the total (or Hildebrand) solubility parameter ( $\delta_t$ ) as the sum of the squares of the HSP d, p, and h components (eq 19).

$$\frac{E}{V} = \frac{E_d}{V} + \frac{E_p}{V} + \frac{E_h}{V} \quad (18)$$

$$\delta_t^2 = \delta_d^2 + \delta_p^2 + \delta_h^2 \quad (19)$$

Applying HSPs to evaluate solution properties is well established.<sup>6,11,12,14,52</sup> Also, HSPs have been used to predict the solution behavior of numerous nanoscale objects such as fullerene,<sup>53</sup> carbon nanotubes,<sup>54</sup> graphene,<sup>55</sup> and biomimetic liquid-crystal hydrogels.<sup>56</sup>

Recently, HSPs were applied by Raynal and Bouteiller<sup>6</sup> to evaluate the behavior of molecular gels using a meta analysis. It revealed that solvents gelated by one gelator had, with few exceptions, similar HSPs.<sup>6</sup> HSPs appear to be an extremely promising tool for analyzing and understanding the factors responsible for the various phases found when a potential gelator and solvent are mixed.<sup>7,8,11,12,14,19,57–59</sup> They have been the basis recently for discoveries pertaining to methods for producing molecular gels from insoluble mixtures<sup>58</sup> and understanding the dynamics of gel formation.<sup>52</sup>

Here, we find that the CGCs of the DBS samples can be correlated with only some of the HSP components (Figure 5B–D). Neither the dispersive nor the polar HSP component is able to predict the gelation ability of DBS in the various solvents investigated (Figure 5B,C). Similar absences of correlation have been reported for solvent mixtures of 12HSA<sup>12</sup> and of a series of pyrenyl-linker-glucono gelators.<sup>58</sup> However, Gao et al.<sup>12</sup> and Yan et al.<sup>58</sup> have shown distinct relationships between  $\delta_h$  and both gelating capacities and CGCs. For 12HSA, clear organogels were reported to form at  $\delta_h < 4.7$  MPa<sup>0.5</sup>, opaque organogels between  $4.7 < \delta_h < 5.1$  MPa<sup>0.5</sup>, and solutions when  $\delta_h > 5.1$  MPa<sup>0.5</sup>.<sup>12</sup> As the CGCs of pyrenyl-linker-glucono gelators increased, so did the  $\delta_h$  values until SAFiN formation was completely inhibited.

However, unlike the cases with 12HSA and pyrenyl-linker-glucono gelators, solutions of DBS occur at intermediate  $\delta_h$  values:  $5.0 < \delta_h < 10.0$  MPa<sup>0.5</sup> (Figure 5D). The CGCs of DBS

mixtures are significantly higher at (and increase between)  $\delta_h$  values for the solvent from 5 to 10 MPa<sup>0.5</sup> compared to the CGCs for  $\delta_h > 12$  MPa<sup>0.5</sup>. Also, when  $\delta_h > 10$  MPa<sup>0.5</sup>, clear gels formed, and when  $\delta_h < 5$  MPa<sup>0.5</sup>, opaque gels resulted. The HSPs aid in understanding which solvents are gelated by DBS and which are not, as well as providing an understanding into why physical aspects of the gels change in different solvents.<sup>11–14</sup>

It was expected that the polar component  $\delta_p$  would not correlate with the gelation phenomenon because it is related to the index of refraction, dielectric constant, and dipole moment (eq 20), none of which show correlations with the assembly of DBS molecules:<sup>60</sup>

$$\delta_p^2 = \frac{12108}{V^2} \frac{\epsilon - 1}{2\epsilon + n_D^2} (n_D^2 + 2)\mu^2 \quad (20)$$

$V$  is the molar volume,  $\epsilon$  is the dielectric constant,  $\mu$  is the dipole moment, and  $n_D$  is the index of refraction.

**Triangular Representation of Hansen Solubility Parameters.** In order to assess better the effect of solvent composition on gelation capacity, Teas diagrams have been used to plot the three HSP parameters (Figure 5E). Teas diagrams employ fractional cohesive energy densities to be distributed more evenly over a triangular chart. In this approach, individual HSPs are converted to an average value by dividing each parameter by their sum (eqs 21–23) and  $\Xi$  is the fraction of the individual HSP components.

$$\Xi_d = \frac{\delta_d}{\delta_d + \delta_h + \delta_p} \quad (21)$$

$$\Xi_p = \frac{\delta_p}{\delta_d + \delta_h + \delta_p} \quad (22)$$

$$\Xi_h = \frac{\delta_h}{\delta_d + \delta_h + \delta_p} \quad (23)$$

The Teas plot in Figure 5C shows a clustering of solvents capable of gelating and another region that remains as solutions. Although Teas plots are useful for detecting general trends, there is no theoretical foundation for calculating the fractions, which assume, incorrectly, that all solvents have the same Hildebrand or total HSP value.<sup>61</sup> Despite this shortcoming, useful information can be derived from Teas plots. In polymer physics, solvents which tend to solubilize a compound of interest cluster in a specific region, the solubility window, on a Teas plot.<sup>20</sup> Although the solubility window for DBS is relatively small, all of the relevant solvents are contained within the lower-right portion of the Teas plot in Figure 5C. Because the DBS solutions fall within the solubility window, it is possible that the clear and opaque gels also may cluster in Hansen space.

**Hansen Space.** The data sets, categorized based on their solubility as solutions, clear gels, and opaque gels, were used to calculate minimal enclosing spheres that contain all points within each category. This estimation was performed using a constrained optimization procedure programmed in Mathematica 9 (Wolfram Research, Champaign IL). The optimization routine uses the NMinimize function to obtain the location of the center of the sphere in terms of values of the dispersive ( $\delta_d$ ), polar ( $\delta_p$ ), and hydrogen-bonding ( $\delta_h$ ) interactions while solving for the smallest possible radius. Using the minimal enclosing spheres, the regions of Hansen spaces were clearly defined (Figure 6). From these spheres, the center and radius of each sphere were determined (Table 1). The NMinimize function was set to

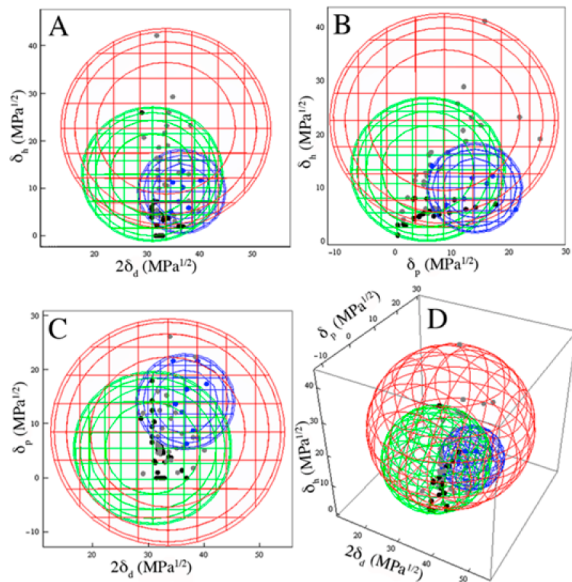


**Figure 6.** Two-dimensional projections (A–C) and a 3D rendering (D) of the Hansen space using minimal enclosing spheres and the appearance at the CGC. The blue sphere encloses DBS solutions, the green sphere encloses opaque gels, and the red sphere encloses clear gels.

**Table 1. Coordinates for the Center of Each Sphere in Hansen Space and the Radius for Each Sphere**

	2δ <sub>d</sub> (MPa <sup>0.5</sup> )	δ <sub>p</sub> (MPa <sup>0.5</sup> )	δ <sub>h</sub> (MPa <sup>0.5</sup> )	radius (MPa <sup>0.5</sup> )
opaque gels	30.7	5.5	13.0	14.2
clear gels	33.4	8.5	22.7	21.1
solutions	36.6	14.1	9.3	9.0

implement the differential evolution optimization method, a robust simple stochastic function minimizer, to reach a numerical global optimum solution.<sup>62</sup> Due to the nature of a global optimum solution, no goodness of fit exists. Therefore, four effective digits of precision were sought in the final results; these criteria were used to halt the iteration process.<sup>62</sup> Obviously, the sizes of the spheres are dependent on the range of solvents chosen. For this reason, it is difficult to determine the exact location/size of the Hansen spheres corresponding to the clear and opaque gels, and important insights are difficult to extract. It is clear that there is excellent confinement of the solutions within the solubility sphere; it effectively excludes the solvents that are gelated (Supporting Information, Figure S5). Similarly, the opaque gel sphere limits the inclusion of solutions but not clear gels, indicating again the importance of directionality in Hansen space and distance. However, the solvents selected suggest that the spheres are not concentric. Instead, the solution sphere resides on the inside edge of the sphere representing the opaque gels, and both reside inside the clear gel sphere. In fact, the definition of sphere radii should be based on data sets for which points occur within each sector of the sphere; that is not the case in the examples of Figure 6.

One important commonly made assumption is that the center of the solution sphere is the HSP of the gelator, DBS in this case. If the coordinates of the solution center are employed, the HSPs for DBS are δ<sub>d</sub> = 18.30 MPa<sup>0.5</sup>, δ<sub>p</sub> = 14.10 MPa<sup>0.5</sup>, and δ<sub>h</sub> = 9.33 MPa<sup>0.5</sup>. Recently, the HSPs for DBS, calculated using a group contribution method, were reported to be δ<sub>d</sub> = 15.89 MPa<sup>0.5</sup>, δ<sub>p</sub> = 3.87 MPa<sup>0.5</sup>, and δ<sub>h</sub> = 18.27 MPa<sup>0.5</sup>.<sup>22</sup> To utilize the group

contribution method, several assumptions must be made, including the fact that the different functional groups that affect the energy of vaporization are additive (i.e., they operate independently). However, it has been shown for complex molecules that this is seldom the case.<sup>48</sup> The HSPs for DBS (δ<sub>d</sub> = 17.6 MPa<sup>0.5</sup>, δ<sub>p</sub> = 8.3 MPa<sup>0.5</sup>, and δ<sub>h</sub> = 10.1 MPa<sup>0.5</sup>), determined using the Y-MB scheme provided in Hansen's HSPiP software<sup>63</sup> corresponded much better to the center of the DBS solution sphere.<sup>64</sup> The Y-MB scheme breaks molecules into their functional groups and estimates various properties. Using the center of the DBS solution sphere (*i*) as the HSP for DBS, the Hansen distances R<sub>ij</sub> between DBS and each of the solvents (*j*) were calculated (eq 24).

$$R_{ij} = (4(\delta_{di} - \delta_{dj})^2 + (\delta_{pi} - \delta_{pj})^2 + (\delta_{hi} - \delta_{hj})^2)^{1/2} \quad (24)$$

If the HSPs of the solvents and DBS are close (i.e., R<sub>ij</sub> < 8.0 MPa<sup>0.5</sup>) (Figure 7A), then a solution will form upon mixing the two. At R<sub>ij</sub> > 8.0 MPa<sup>0.5</sup>, there was no correlation between the distance in Hansen space and the likelihood of forming a clear or opaque gel. This suggests that the magnitude of the vector between the HSP of a solvent and of DBS alone does not accurately predict the interactions driving self-assembly. The question arises, then, as to whether the direction of the R<sub>ij</sub> vector is also a factor influencing the predictability of the gel state. In an attempt to gain a better understanding of these factors, the R<sub>ij</sub> vector was dissected to assess the distance between DBS (i.e., center of the solution sphere (Figure 6)) and each solvent (eqs 25–27)).

$$\Delta 2\delta_d = (2\delta_{di}) - (2\delta_{dj}) \quad (25)$$

$$\Delta \delta_p = \delta_{pi} - \delta_{pj} \quad (26)$$

$$\Delta \delta_h = \delta_{hi} - \delta_{hj} \quad (27)$$

Δ2δ<sub>d</sub> is the magnitude difference between the dispersive components of the HSP for a solvent (*j*) and the gelator (*i*); a multiple of 2 is used for consistency between Hansen space and distance calculations. Δδ<sub>p</sub> is the magnitude difference between the polar components, and Δδ<sub>h</sub> is the magnitude difference of the hydrogen-bonding component of the HSPs.

By observing the effect of only two of the three parameters simultaneously, several important trends become obvious (Figure 7B–D). First, solvents in which DBS formed solutions are closest to the (0, 0) axis in each plot (Figure 7B–D). By dissecting the role of Δδ<sub>p</sub> and Δ2δ<sub>d</sub> only, it appears that clear organogels are more likely to occur at intermediate distances from the HSP of DBS, and opaque gels occur within a radius farther from the HSP center of DBS (Figure 7B). However, this combination does not include the δ<sub>h</sub> parameter of the gelator. When the roles of Δδ<sub>h</sub> and Δ2δ<sub>d</sub> of the solvents are observed, while ignoring the influence of δ<sub>p</sub>, an interesting trend emerges (Figure 7C). Opaque gels tend to form in solvents when Δδ<sub>h</sub> > 0 (i.e., when δ<sub>h</sub> for the solvent is less than that of DBS). Conversely, clear DBS gels form in solvents when Δδ<sub>h</sub> < 0 (i.e., when δ<sub>h</sub> for the solvent is higher than that of DBS). This insight allows a more accurate prediction of when an untested solvent will (and will not) provide the desired molecular gel characteristics. These trends are observed also when combining Δδ<sub>h</sub> and Δδ<sub>p</sub> (while ignoring Δ2δ<sub>d</sub>), although in this case there is a slight overlap (or transition) between the two phases in the region, 2.0 < Δδ<sub>h</sub> < -1.0 MPa<sup>0.5</sup> (Figure 7D).

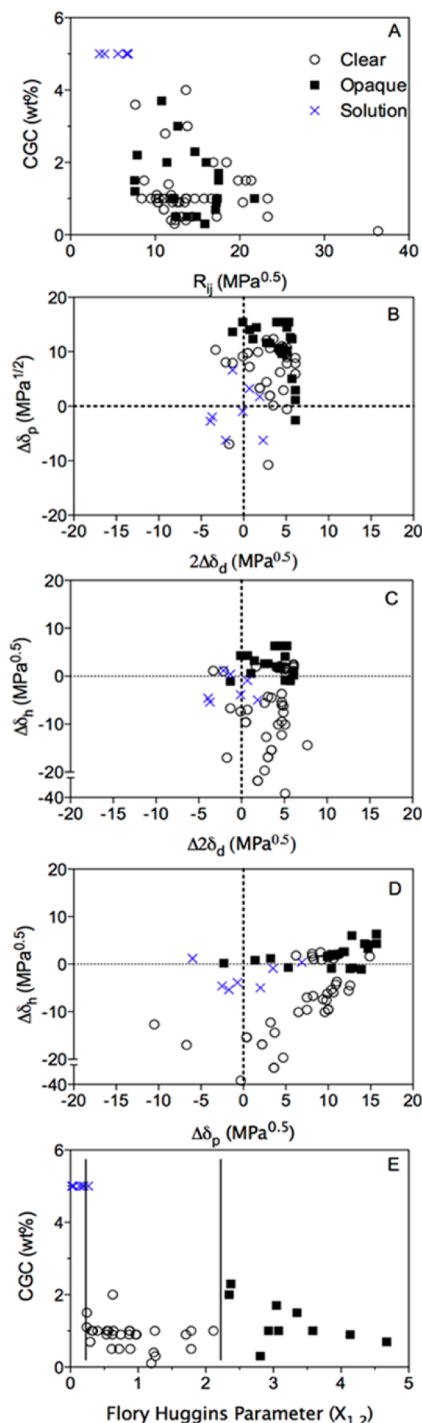


**Figure 7.** Distances in Hansen space (A) between the DBS solution center ( $\delta_d = 18.3 \text{ MPa}^{0.5}$ ,  $\delta_p = 14.1 \text{ MPa}^{0.5}$ , and  $\delta_h = 9.33 \text{ MPa}^{0.5}$ ) from Figure 6 and each solvent Hansen parameter. Two-dimensional projections of the distance between the solvent and DBS polar ( $\Delta\delta_p$ ) (B), dispersive ( $\Delta 2\delta_d$ ) (C), and hydrogen-bonding ( $\Delta\delta_h$ ) (D) Hansen parameters and the Flory–Huggins interaction parameters ( $\chi_{12}$ ) (E).

**Flory–Huggins Interaction Parameter.** The Flory–Huggins interaction parameter ( $\chi_{12}$ ) is traditionally derived from the Hildebrand solubility parameters of the solvent ( $\delta_1$ ) and gelator ( $\delta_2$ ; usually a polymer) and the solvent molar volume ( $V_1$ ) (eq 28).<sup>7</sup>

$$\chi_{12} = \frac{V_1(\delta_2 - \delta_1)^2}{RT} \quad (28)$$

However, because the Hildebrand solubility parameter of DBS is unavailable, an extension of the Flory–Huggins equation proposed by Lindqvist et al. was utilized (eq 29).<sup>16</sup>

$$\begin{aligned} \chi_{12} = \alpha^* \frac{V_1}{RT} [ & (\delta_{di} - \delta_{dj})^2 + 0.25(\delta_{pi} - \delta_{pj})^2 \\ & + 0.25(\delta_{hi} - \delta_{hj})^2 ] \end{aligned} \quad (29)$$

$\alpha^*$  is a constant for a volume-based combination term ( $\alpha^* = 0.6$ ), and the Hansen parameters for DBS are obtained from the center of the solution sphere (Table 1).<sup>16</sup>

Flory<sup>65–67</sup> and Huggins<sup>24</sup> first utilized the enthalpy and entropy of mixing of long-chain molecules, assuming that polymer segments and solvent molecules occupied single lattice points. Note that the interaction parameter must be determined in dilute solutions, as is the case for most of the DBS molecular gels. A major advantage of the Flory–Huggins parameter over some of the others is that it accounts for differences in molecular sizes that contribute to changes in the entropy of mixing. Empirically, it is extremely effective at differentiating the solvent dependence on the different phases of DBS-solvent mixtures (Figure 7E). Consistent with solution theory, which states that decreasing values of  $\chi_{12}$  increase the tendency of dissolution, DBS solutions were found at low values of  $\chi_{12}$ .<sup>7</sup> Clear gels were observed in solvents with intermediate  $\chi_{12}$  values, and opaque gels were obtained when  $\chi_{12}$  values were high. These trends are identical to those observed by Fan et al. for systems composed of melamine and di(2-ethylhexyl) phosphoric acid as a two-part gelator.<sup>7</sup>

**Conclusions from Thermodynamically Derived Solvent Parameters.** HSPs show trends similar to those found by application of the  $\alpha$  and SA parameters. The ability of the solvent to undergo strong hydrogen bonding alters the ability of the gelator to establish a hydrogen-bonded network; another example was found in L-lysine-derived gelators.<sup>41</sup> Solvents tend to cluster in Hansen space depending on whether solutions or clear or opaque gels prevail, and the arrangement of these Hansen spheres is not concentric based on the selected solvents. As mentioned above, this nonconcentric arrangement may be a caveat of solvent selection, and only when the solvent points are fairly evenly distributed in Hansen space can one make a firm statement about the concentric nature. However, based on the solvents selected in this study, the directionality of the vector defined by the DBS and solvent HSPs is extremely important. In addition, the Flory–Huggins interaction parameters predict the final structures, which form when DBS sols are cooled below the DBS melting temperature.

**Classification of Mixtures Using Cluster Analysis of Dual Solvent Parameter Data.** As previously mentioned, because self-assembly in molecular gels is influenced by both solvent–solute interactions and bulk solvent properties, it is not possible to know a priori which solvent parameters are most important for screening the probability of gelation of a solvent by a selected molecular gelator. Individual solvent parameters, including dielectric constants,<sup>15,68</sup> Hildebrand solubility parameters,<sup>6,7</sup>  $E_T(30)$  parameters,<sup>17,18</sup> solvent polarity (polarizability (SPP)), solvent basicity (SB) and solvent acidity (SA),<sup>18</sup> Kamlet–Taft parameters,<sup>15</sup> and the Flory–Huggins parameter<sup>16</sup> have been applied extensively in an ad hoc manner with mixed success to predict gelator behavior. Unfortunately, the most widely

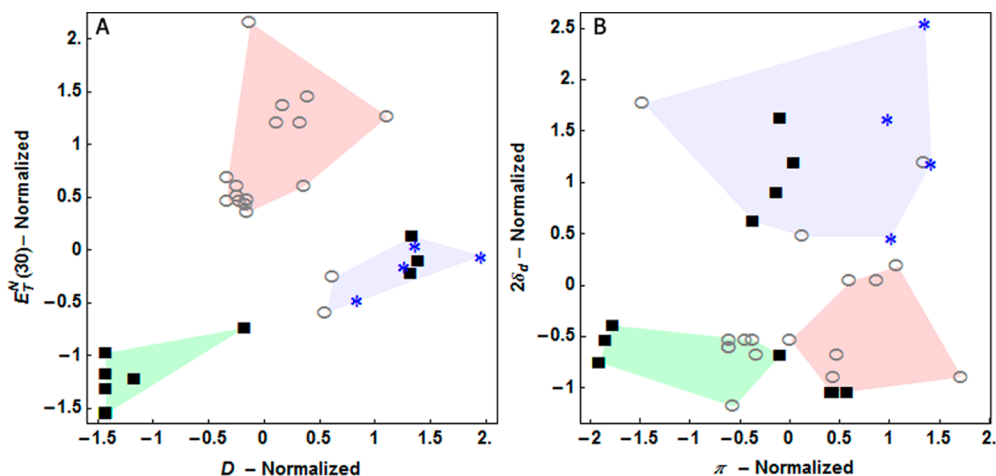


**Figure 8.** Classification of DBS mixtures based on cluster analyses using pairs of solvent parameter values. (A)  $E_T^n(30)$  vs  $D$  (85% correct classification) and (B)  $2\delta_d$  vs  $\pi$  (48% correct classification). Circles are for clear gels, squares are for opaque gels, and stars are for solutions.

**Table 2. Classification of DBS–Solvent Mixtures Based on Cluster Analyses Using Two Solvent Parameters and the Degree of Their Predictability as a Percentage<sup>a</sup>**

	$\log P$	$D$	$E_T^n(30)$	$\alpha$	$\beta$	$\pi$	SPP	SB	SA	$\delta_d$	$\delta_p$	$\delta_h$
$\log P$		70	58	79	67	58	66	69	75	64	61	58
$D$			85	79	79	67	69	66	75	70	67	82
$E_T^n(30)$				82	73	70	81	69	69	73	70	61
$\alpha$					76	67	78	72	69	76	82	64
$\beta$						58	72	66	75	70	64	67
$\pi$							50	53	50	48	48	48
SPP								66	53	72	66	59
SB									72	69	66	
SA										75	78	69
$\delta_d$											52	52
$\delta_p$												55
$\delta_h$												

<sup>a</sup>Solvent parameters were preselected with a minimum of 32 solvents. Units are as described in the text.

available solvent parameters (i.e., macroscopic measurements of dielectric constants,  $\log P$ , RI, etc.) show the poorest correlations with the likelihood of DBS self-assembling into linear aggregates. Recently, grouping solvents by statistical analysis to screen the assembly of single crystal polymorphs has shown tremendous promise.<sup>5</sup> To assess the predictive ability of solvent parameter pair combinations on the mode of assembly for DBS, a cluster analysis was carried out. This unsupervised learning technique allows the organization of a collection of data points, in our case, solvent parameter combinations, into clusters based on a distance or dissimilarity function.<sup>69</sup> The capability of the solvent parameter combinations to predict gelator behavior has been evaluated here based on their probability to group data points pertaining to a single type of outcome (solution, clear gel, or opaque gel) into distinctive clusters.

Only solvent parameters that were available for the majority (33) of our solvents were utilized in this cluster analysis to increase the likelihood of widespread applicability. To avoid larger-scale parameters to dominate others,<sup>69</sup> each was standardized by mean removal and variance scaling prior to the classification stage. Cluster analysis was then performed using a k-medoids algorithm (related to the k-means algorithm).<sup>70</sup> This clustering technique was programmed in Mathematica 9 using the FindClusters function under the Optimize method, which through an iterative approach finds a local optimum clustering.

The Euclidean distance (i.e., square root of the sums of the squares of the differences between the coordinates of the points in each dimension)<sup>71</sup> was used to reflect dissimilarity between two data points. The utilization of centroid-based algorithms, such as the k-medoids, for classification requires specifying in advance the number of output clusters. In our case, the number of output clusters was set to 3, which accounts for all possible outcomes—solution, clear gel, or opaque gel—for our samples.

Calculating the smallest convex set that contained all points pertaining to a cluster using the computational geometry package in Mathematica 9 plotted the output clusters. The data points, differentially identified based on the gel structure, were overlaid on each cluster area to emphasize correspondence (Figure 8). The predictive ability of the solvent parameter pair combinations was evaluated based on the percentage of correct grouping. Because the DBS mixtures are being placed into three different cluster states, a random result would place one-third of the solvents into the correct cluster. Several of the solvent parameter pairings did not cluster the solvents effectively into their appropriate group (Table 2). For example, clustering solvents based on their  $\pi$  parameter and the dispersive Hansen solubility parameter ( $\delta_p$ ) placed only 48% of the solvents into their appropriate cluster (Figure 8B). However, clustering the solvents based on certain pairings increased the percentage of correct classification to well above 80% and even as high as 85% (i.e.,  $D$

and  $E_T^n(30)$  parameters) (Figure 8A). What is most intriguing about this cluster analysis is that two parameters that individually do not correlate DBS assembly do so well when paired. A probable reason for this is that two parameters typify polarity more completely than individual solvent properties. Thus, using cluster analysis may lead to insights about the factors responsible for molecular gelator (and other forms of) self-assembly from more easily obtained solvent data than that from the more complex parameters.

## ■ OVERALL CONCLUSIONS

Using DBS as the molecular gelator, direct comparisons of solvent–solute parameters and the physical properties of gels as well as analyses of the bases upon which the parameters are formulated can be used to gain a better understanding of how such data treatments should be applied to systems involving molecular gels and which structural parts of a molecular gelator are important in its aggregation, nucleation, and SAFiN-forming events leading to gelation.

Opaque DBS gels tended to be weaker (i.e., lower  $G'$  and lower yield stress values) and composed of thicker bundles of fibers than the transparent gels. Although polarity (as measured by the partitioning coefficients, Henry's law constants, static relative permittivity, refractive index, and the  $E_T(30)$  parameters) of the solvent plays a role in the final state of the DBS–solvent mixtures, it is difficult to draw general conclusions other than clear gels more likely to form in higher-polarity solvents than in lower-polarity solvents. Analyses of the data using the solvatochromic parameters derived by Kamlet and Taft and by Catalan et al. strongly suggest that although the polarity of a solvent is important, its ability to accept or donate a hydrogen bond is much more consequential to determining whether the addition of DBS will result in a solution, a clear gel, or an opaque gel.

As demonstrated by the observation that Hildebrand parameters are ineffective at correlating the nature of the DBS phases, the thermodynamically derived parameters must be separated into individual Hansen solubility parameters. When so analyzed, the different phases tend to cluster in Hansen space. They are more sensitive to the hydrogen-bonding HSP component than to the polar and dispersive HSP components. Unlike polymers, which are very sensitive to the distance in Hansen space between their HSP and that of a solvent but much less so to the vector connecting the two points, the phases of the DBS–solvent systems are sensitive to both (e.g., opaque gels form when the solvent has a lower hydrogen-bonding HSP than does DBS). This observation is consistent with conclusions derived from solvatochromic-based measurements, corresponding to opaque gels resulting when DBS cannot accept a hydrogen bond. The Flory–Huggins parameter is extremely efficient at clustering the different DBS solution and gel states: low values of the interaction parameters lead to solutions, and high values of the interaction parameter lead to opaque gels; clear gels are found when values of the interaction parameter are in the intermediate range. Finally, cluster analysis or pattern identification techniques may allow commonly available measures of solvent polarity that are individually ineffective at predicting the self-assembly of molecular gel formation, to be combined to identify with greater confidence which solvents are capable of being gelated a priori.

We emphasize that DBS has been used here for demonstrative purposes. However, these parameters may be applied to all molecular gelations and treatments, and employing different

molecular gelators will be required to build confidence that the treatments employed and comparisons made here are generally applicable. Regardless, a blueprint for how to proceed in such studies has been outlined. It is hoped that we and others will supply the data and analyses to determine whether the sought-after generality can be achieved.

## ■ ASSOCIATED CONTENT

### § Supporting Information

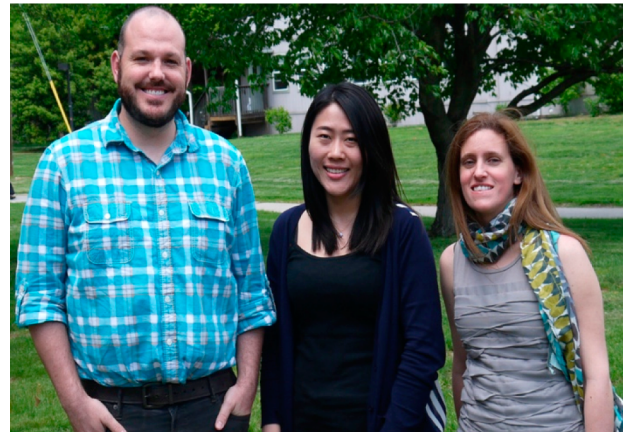
Solvent purities, critical gelator concentrations, and visual appearances of the gels. Solubility parameters obtained from the literature. Schematic diagram of the rheological molds. Brightfield micrographs. FTIR spectromicrographs. Average rheological stress sweeps for opaque and clear gels, and distances from the centers of the solubility spheres (Figure S5) are included. This material is available free of charge via the Internet at <http://pubs.acs.org>.

## ■ AUTHOR INFORMATION

### Notes

The authors declare no competing financial interest.

### Biographies



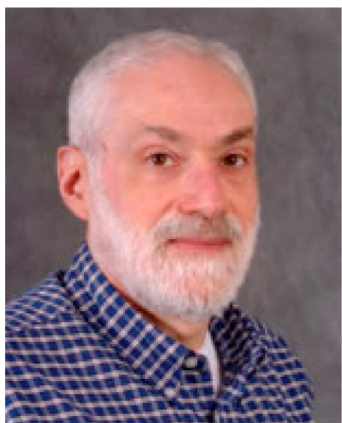
Left to Right: Michael A. Rogers, Yaqi Lan, and Maria G. Corradini

Michael A. Rogers received an MSc under the supervision of Dr. H. Douglas Goff in 2005 and a Ph.D. under the mentorship of Drs. Alejandro G. Marangoni and Amanda J. Wright in 2008 from the University of Guelph. From 2008 to 2011, he was an assistant professor at the University of Saskatchewan, and the Natural Sciences and Engineering Research Council of Canada (NSERC) funded his research focusing primarily on molecular gels. In 2011, he joined Rutgers University, The State University of New Jersey, in the Department of Food Science, and in 2012, he was appointed the Director of the Center for Gastrointestinal Physiology at the New Jersey Institute of Food, Nutrition, and Health (IFNH). In 2013, he won the Directors Award for Scientific Excellence from IFNH. He has been awarded two patents on molecular gels as edible fat replacers and as phase-selective sorbent xerogels to be used as reclamation agents for oil spills. His research interests are the self-assembly of fibrillar aggregates in molecular gels, biomaterials, and biomimics and the biophysics of digestion.

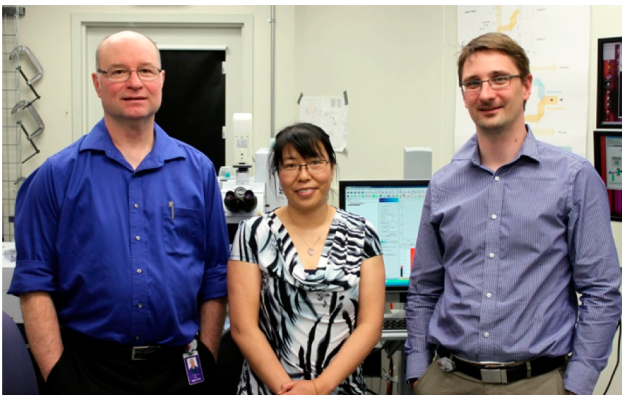
Yaqi Lan received her B.A. degree in food science from Jiangnan University, China in 2011. She is currently a Ph.D. candidate under the supervision of Dr. Michael Rogers and a recipient of an Excellence Fellowship at Rutgers University, the State University of New Jersey.

Maria G. Corradini received her Ph.D. in 2004 from the Department of Food Science, University of Massachusetts—Amherst. Currently she holds a position as assistant research professor at Rutgers, The State

University of New Jersey. Her research interests mainly focus on modeling nonlinear kinetics and photophysics.



Richard G. Weiss received an Sc.B. degree from Brown University and M.S. and Ph.D. degrees from the University of Connecticut under the mentorship of Eugene I. Snyder. He was an NIH Postdoctoral Fellow with George S. Hammond at the California Institute of Technology and a visiting assistant professor and National Academy of Sciences Overseas Fellow at the Instituto de Química of the Universidade de São Paulo in Brazil. He has been a member of the faculty of Georgetown University since 1974. He is a Fellow of IUPAC and a member of the Brazilian Academy of Sciences and received a doctorate honoris causa from Université de Bordeaux 1. He is a senior editor of the ACS journal *Langmuir* and a member of the editorial advisory board of the *Journal of the Brazilian Chemical Society*. His research interests include investigations of photochemical, photophysical, and thermal reactions of molecules in anisotropic environments and the development and application of new molecular and polymer gels, ionic liquids, and ionic liquid crystals.



Left to Right: Tim E. May, Xia Liu, and Ferenc Borondics

Tim May has been a staff scientist at the Canadian Light Source since 2000, where he designed and operates two infrared synchrotron beamlines. His primary interests are in developing optical interfaces for diffraction-limited spectral imaging for biological and materials research. His prior synchrotron work was at the University of Wisconsin after obtaining a physics M.Sc. from Case Western Reserve in 1979.

Xia Liu received her B.Sc. and M.Sc. degrees from Liaocheng University and the University of Science and Technology of China, respectively. She did her Ph.D. with Prof. Ronald Steer at the University of Saskatchewan and received her degree in 2009. Then she did postdoctoral research with Prof. Michael Woodside at the University of Alberta and National Institute of Nanotechnology at Edmonton. In 2012, she joined the Canadian Light Source Inc. as a science associate of the mid-IR beamline.

Ferenc Borondics was awarded his master's degree in chemistry with special focus on molecular structure determination and chemical informatics from the Eötvös Loránd University in Budapest, Hungary in 2002. From the same institution he received a Ph.D. degree in inorganic chemistry in 2007 under the supervision of Katalin Kamarás. From 2007 to 2008, he was a postdoctoral fellow at the Lawrence Berkeley National Laboratory at the Advanced Light Source Division working with Michael C. Martin, and from 2008 to 2010, he was in the Chemical Sciences Division under the supervision of Miquel B. Salmeron. Currently, he is the beamline scientist for the mid-IR spectromicroscopy beamline at the Canadian Light Source in Saskatoon, Saskatchewan. His research interests include infrared technique development and the study of carbon nanomaterials.

## ACKNOWLEDGMENTS

M.A.R. acknowledges the USDA HATCH Program, through the New Jersey Agriculture Research Station (NJAES) for partial funding of this project. A portion of the research described in this article was performed at the Canadian Light Source, which is supported by NSERC, NRC, CIHR, and the University of Saskatchewan. We are grateful to Tim May (CLS) for beamline design and construction and for constant help with beamline upkeep. R.G.W. thanks the U.S. National Science Foundation (grant CHE-1147353) and the Gulf of Mexico Research Initiative for their support of the research at Georgetown. We also acknowledge Dr. Steven Abbott for in-depth discussions on the application of Hansen solubility parameters.

## REFERENCES

- (1) Weiss, R. G. The Past, Present, and Future of Molecular Gels. What Is the Status of the Field, and Where Is It Going? *J. Am. Chem. Soc.* **2014**, *136*, 7519–7530.
- (2) van Esch, J. H. We can design molecular, but do we understand them? *Langmuir* **2008**, *25*, 8392–8394.
- (3) Jonkheijm, P.; van der Schoot, P.; Schenning, A. P. H. J.; Meijer, E. W. Probing the Solvent-Assisted Nucleation Pathway in Chemical Self-Assembly. *Science* **2006**, *313*, 80–83.
- (4) Katritzky, A. R.; Fara, D. C.; Yang, H.; Tämm, K.; Tamm, T.; Karelson, M. Quantitative Measures of Solvent Polarity. *Chem. Rev.* **2004**, *104*, 175–198.
- (5) Gu, C.-H.; Li, H.; Gandhi, R. B.; Raghavan, K. Grouping solvents by statistical analysis of solvent property parameters: implication to polymorph screening. *Int. J. Pharm.* **2004**, *283*, 117–125.
- (6) Raynal, M.; Bouteiller, L. Organogel Formation Rationalized by Hansen Solubility Parameters. *Chem. Commun.* **2011**, *47*, 8271–8273.
- (7) Fan, K.; Niu, L.; Li, J.; Feng, R.; Qu, R.; Liu, T.; Song, J. Application of solubility theory in bi-component hydrogels of melamine with di(2-ethylhexyl) phosphoric acid. *Soft Matter* **2013**, *9*, 3057–3062.
- (8) Niu, L.; Song, J.; Li, J.; Tao, N.; Lu, M.; Fan, K. Solvent effects on the gelation performance of melamine and 2-ethylhexylphosphoric acid mono-2-ethylhexyl ester in water–organic mixtures. *Soft Matter* **2013**, *9*, 7780–7786.
- (9) Kaszynska, J.; Lapinski, A.; Bielejewski, M.; Luboradzki, R.; Trittgoc, J. On the relation between the solvent parameters and the physical properties of methyl-4,6-O-benzylidene- $\alpha$ -D-glucopyranoside organogels. *Tetrahedron* **2012**, *68*, 3803–3810.
- (10) Lide, D. R. *CRC Handbook of Chemistry and Physics*; CRC Press: Boca Raton, FL, 2005.
- (11) Gao, J.; Wu, S.; Emge, T.; Rogers, M. A. Nanoscale and Microscale Structural Changes Alter the Critical Gelator Concentration of Molecular Gels in Organic Solvents. *Cryst. Eng. Commun.* **2013**, *15*, 4507–4515.
- (12) Gao, J.; Wu, S.; Rogers, M. A. Harnessing Hansen Solubility Parameters to Predict Organogel Formation. *J. Mater. Chem.* **2012**, *22*, 12651–12658.

- (13) Wu, S.; Gao, J.; Emge, T.; Rogers, M. A. Solvent Induced Polymorphic Nanoscale Transitions for 12-Hydroxyoctadecanoic Acid Molecular Gels. *Cryst. Growth Des.* **2013**, *13*, 1360–1366.
- (14) Wu, S.; Gao, J.; Emge, T.; Rogers, M. A. Influence of solvent on the supramolecular architectures in molecular gels. *Soft Matter* **2013**, *9*, 5942–5950.
- (15) Hirst, A. R.; Smith, D. K. Solvent Effects on Supramolecular Gel-Phase Materials: Two-Component Dendritic Gel. *Langmuir* **2004**, *20*, 10851–10857.
- (16) Lindvig, T.; Michelsen, M. L.; Kontogeorgis, G. M. A Flory–Huggins model based on the Hansen solubility parameters. *Fluid Phase Equilif.* **2002**, *203*, 247–260.
- (17) Bielejewski, M.; Łapiński, A.; Luboradzki, R.; Tritt-Goc, J. Solvent effect on 1,2-O-(1-ethylpropylidene)- $\alpha$ -D-glucofuranose organogels properties. *Langmuir* **2009**, *25*, 8274–8279.
- (18) Zhu, G.; Dordick, J. S. Solvent Effect on Organogel Formation by Low Molecular Weight Molecules. *Chem. Mater.* **2006**, *18*, 5988–5995.
- (19) Liu, S.; Yu, W.; Zhou, C. Solvents effects in the formation and viscoelasticity of DBS organogels. *Soft Matter* **2013**, *2013*, 864–874.
- (20) Hansen, C. M. *Hansen Solubility Parameters*, 2nd ed.; CRC Press: Boca Raton, FL, 2007.
- (21) Terech, P.; Pasquier, D.; Bordas, V.; Rossat, C. Rheological properties and structural correlations in molecular gels. *Langmuir* **2000**, *16*, 4485–4494.
- (22) Lui, S.; Yu, W.; Zhou, C. Solvents effects in the formation and viscoelasticity of DBS organogels. *Soft Matter* **2013**, *9*, 864–874.
- (23) Terech, P.; Weiss, R. G. Low Molecular Mass Gelators of Organic Liquids and the Properties of Their Gels. *Chem. Rev.* **1997**, *97*, 3133–3159.
- (24) Huggins, M. L. Solutions of long chain compounds. *J. Chem. Phys.* **1941**, *9*, 440.
- (25) Kentsis, A.; Borden, K. L. B. Physical Mechanisms and Biological Significance of Supramolecular Protein Self-Assembly. *Curr. Protein Pept. Sci.* **2004**, *5*, 125–134.
- (26) Liu, W.; Prausnitz, J. M.; Blanch, H. W. Amyloid Fibril Formation by Peptide LYS (11–36) in Aqueous Trifluoroethanol. *Biomacromolecules* **2004**, *5*, 1818–1823.
- (27) Trann, T. T.; Tran, P. H.; Park, J. B.; Lee, B. J. Effects of solvents and crystallization conditions on the polymorphic behaviors and dissolution rates of valsartan. *Arch. Pharm. Res.* **2012**, *35*, 1223–1230.
- (28) Sangster, J. Octanol-Water partition coefficients of simple organic compounds. *J. Phys. Chem. Ref. Data* **1989**, *18*, 1111–1227.
- (29) PubChem Compound Summaries. <http://www.ncbi.nlm.nih.gov/guide/> (accessed 12/23/13).
- (30) Staudinger, J.; Robers, P. V. A critical compilation of Henry's law constant temperature dependence relation for organic compounds in dilute aqueous solutions. *Chemosphere* **2001**, *44*, 561–576.
- (31) Reichardt, C. *Solvents and Solvent Effects in Organic Chemistry*, 2nd ed.; VCH: Weinheim, Germany, 1988.
- (32) Weast, R. C.; Astle, M. J. *CRC Handbook of Data on Organic Compounds*; CRC Press: Boca Raton, FL, 1986.
- (33) Reichardt, C. *Solvents and Solvent Effects in Organic Chemistry*, 3rd ed.; Wiley-VCH: Marburg, Germany, 2004.
- (34) Reichardt, C. Polarity of ionic liquids determined empirically by means of solvatochromic pyridinium N-phenolate betaine dyes. *Green Chem.* **2005**, *7*, 339–351.
- (35) Dimroth, K.; Reichardt, C.; Siepmann, T.; Bohlmann, F. Über Pyridinium-N-phenol-betaine und ihre Verwendung zur Charakterisierung der Polarität von Lösungsmitteln. *Liebigs Ann. Chem.* **1963**, *661*, 1–37.
- (36) Kamlet, M. J.; Abboud, J. L.; Taft, R. W. The Solvatochromic Comparison Method. 6. The  $\pi^*$  Scale of Solvent Polarities. *J. Am. Chem. Soc.* **1977**, *99*, 6027–6038.
- (37) Kamlet, M. J.; Taft, R. W. The Solvatochromic Comparison Method. I. The  $\beta$  Scale of Solvent Hydrogen-Bond Acceptor (HBA) Basicities. *J. Am. Chem. Soc.* **1976**, *98*, 377–383.
- (38) Taft, R. W.; Kamlet, M. J. The Solvatochromic Comparison Method. 2. The  $\alpha$ -Scale of Solvent Hydrogen-Bond Donor (HBD) Acidities. *J. Am. Chem. Soc.* **1976**, *98*, 2886–2894.
- (39) Wyatt, V. T.; Bush, B.; Lu, J.; Hallett, J. P.; Liotta, C. L.; Eckert, C. A. Determination of solvatochromic solvent parameters for the characterization of gas-expanded liquids. *J. Supercrit. Fluids* **2005**, *36*, 16–22.
- (40) Lagalante, A. E.; Wood, C.; Clarke, A. M.; Bruno, T. J. Kamlet-Taft solvatochromic parameters for 25 glycol ether solvents and glycol ether aqueous solutions. *J. Solution Chem.* **1998**, *27*, 887–900.
- (41) Edwards, W.; Lagadec, C. A.; Smith, D. K. Solvent-gelator interactions—using empirical solvent parameters to better understand the self-assembly of gel-phase materials. *Soft Matter* **2011**, *7*, 110–117.
- (42) Catalan, J.; Lopez, V.; Perez, P.; Martin-Willamil, R.; Rodriguez, J.-G. Progress towards a generalized solvent polarity scale: the solvatochromism of 2-(Dimethylamino)-7-nitrofluorene and its homomorph 2-Fluoro-7-nitrofluorene. *Liebigs Ann. Chem.* **1995**, *1995*, 241–252.
- (43) Catalan, J.; Diaz, C.; Lopez, C.; Perez, P.; de Paz, J.-L. G.; Rodriguez, J.-G. A Generalized Solvent Basicity Scale: The Solvatochromism of 5-Nitroindoline and Its Homomorph 1-Methyl-5-nitroindoline. *Liebigs Ann. Chem.* **1996**, *1996*, 1785–1794.
- (44) Catalan, J.; Diaz, C. A Generalized Solvent Acidity Scale: The Solvatochromism of o-tert-Butylstilbazonium Betaine Dye and Its Homomorph o,o'-Di-tert-butylstilbazonium Betaine Dye. *Liebigs Ann. Chem.* **1997**, *1997*, 1941–1949.
- (45) Catalan, J. Towards the gas-phase UV/VIS absorption spectrum of C<sub>60</sub>. *Chem. Phys. Lett.* **1994**, *223*, 159–161.
- (46) Hildebrand, J. H.; Scott, R. L. *The Solubility of Nonelectrolytes*, 3rd ed.; Dover Publications: Reinhold, NY, 1959.
- (47) Scatchard, G. Equilibrium in nonelectrolyte mixtures. *Chem. Rev.* **1949**, *44*, 7–35.
- (48) Grulke, E. A. *Solubility Parameter Values*, 4th ed.; John Wiley & Sons: New York, 2005.
- (49) Barton, A. F. M. Solubility Parameters. *Chem. Rev.* **1975**, *75*, 731–753.
- (50) Greaves, Y. L.; Drummond, C. J. Solvent nanostructure, the solvophobic effect and amphiphile self-assembly in ionic liquids. *Chem. Soc. Rev.* **2013**, *42*, 1096–1120.
- (51) Hansen, C. M. 50 years with solubility parameters—past and future. *Prog. Org. Coat.* **2004**, *51*, 77–84.
- (52) Diehn, K. K.; Oh, H.; Hashemipour, R.; Weiss, R. G.; Raghavan, S. R. The Physical Chemistry of Molecular Gels: Insights into Self-Assembly-Based Organogelation and its Kinetics via Hansen Solubility Parameters. *Soft Matter* **2014**, *10*, 2632–2640.
- (53) Hansen, C. M.; Smith, A. L. Using Hansen solubility parameters to correlate solubility of C<sub>60</sub> fullerene in organic solvents and in polymers. *Carbon* **2004**, *42*, 1591–1597.
- (54) Detrich, S.; Nagy, J. B.; Mekhalif, Z.; Delhalle, J. Surface state of carbon nanotubes and Hansen solubility parameters. *J. Nanosci. Nanotechnol.* **2009**, *9*, 6015–6025.
- (55) Hernandez, Y.; Lotya, M.; Rickard, D.; Bergin, S. D.; Coleman, J. N. Measurement of Multicomponent Solubility Parameters for Graphene Facilitates Solvent Discovery. *Langmuir* **2009**, *26*, 3208–3213.
- (56) Batra, D.; Hay, D. N. T.; Firestone, M. A. Formation of a Biomimetic, Liquid-Crystalline Hydrogel by Self-Assembly and Polymerization of an Ionic Liquid. *Chem. Mater.* **2007**, *19*, 4423–4431.
- (57) Yan, N.; Xu, Z.; Diehn, K. K.; Raghavan, S. R.; Fang, J.; Weiss, R. G. How Do Liquid Mixtures Solubilize Insoluble Gelators? Self-Assembly Properties of Pyrenyl-Linker-Glucono Gelators in Tetrahydrofuran-Water Mixtures. *J. Am. Chem. Soc.* **2013**, *135*, 8989–8999.
- (58) Yan, N.; Xu, Z.; Diehn, K. K.; Raghavan, S. R.; Fang, Y.; Weiss, R. G. Pyrenyl-Linker-Glucono Gelators. Correlations of Gel Properties with Gelator Structures and Characterization of Solvent Effects. *Langmuir* **2013**, *29*, 793–805.
- (59) Edwards, W.; Smith, D. K. Dynamic evolving two component supramolecular gel-hierarchical control over component selection in complex mixtures. *J. Am. Chem. Soc.* **2013**, *135*, 5911–5920.
- (60) Zeng, W.; Du, Y.; Xue, Y.; Frisch, H. L. Solubility Parameters. In *Physical Properties of Polymers Handbook*, 2nd ed., Mark, J. E., Ed.; Springer: New York, 2007; pp 289–302.

- (61) Bonnet, J.; Suissa, G.; Raynal, M.; Bouteiller, L. Organogel formation rationalized by Hansen solubility parameters: dos and don'ts. *Soft Matter* **2014**, *10*, 3154–3160.
- (62) Storn, R.; Price, K. Differential Evolution – A Simple and Efficient Heuristic for Global Optimization over Continuous Spaces. *J. Global Optim.* **1997**, *11*, 341–359.
- (63) Hansen, C. M. *Hansen Solubility Parameters in Practice (HSPiP)*. www.Hansen-Solubility.com (accessed August, 2013).
- (64) Abbott, S. Personal communication, 2012.
- (65) Flory, P. J. *Principles of Polymer Chemistry*; Cornell University Press: Ithaca, NY, 1953.
- (66) Flory, P. J.; Rehner, J. Statistical Theory of Chain Configuration and Physical Properties of High Polymers. *Ann. NY Acad. Sci.* **1943**, *44*, 419–429.
- (67) Flory, P. J. Thermodynamics of high polymer solutions. *J. Chem. Phys.* **1941**, *9*, 660–661.
- (68) Aggeli, A.; Bell, M.; Boden, M.; Keen, J. N.; Knowles, P. F.; McLeish, T. C. B.; Pitkeathly, M.; Radford, S. E. Responsive gels formed by the spontaneous self-assembly of peptides into polymeric  $\beta$ -sheet tapes. *Nature* **1997**, *386*, 259–262.
- (69) Jain, A. K.; Murty, M. N.; Flynn, P. J. Data Clustering: A Review. *ACM Comput. Surv.* **1999**, *31*, 264–323.
- (70) Velmurugan, T.; Santhanam, T. Computational Complexity between K-Means and K-Medoids Clustering Algorithms for Normal and Uniform Distributions of Data Points. *J. Comput. Sci.* **2010**, *6*, 363–368.
- (71) Rajaraman, A.; Leskovec, J.; Ullman, J. D. *Mining of Massive Datasets*; Cambridge University Press: Cambridge, UK, 2010.